


Article

Synthesis of Two Novels-Shaped Dibenzo[c,l] Chrysene Derivatives, Crystal Structure, and the Evaluation of their Photophysical Properties

Tetsuji Moriguchi ^{1,*} , Daichi Tabuchi ¹, Daisuke Yakeya ¹, Akihiko Tsuge ¹ and Venkataprasad Jalli ²

¹ Department of Applied Chemistry, Faculty of Engineering, Kyushu Institute of Technology, Kitakyushu, Fukuoka 804-8550, Japan; cococo_cococo0520@gmail.com (D.T.); yakeya_d@yahoo.co.jp (D.Y.); tsuge@che.kyutech.ac.jp (A.T.)

² Sankar Foundation, Research and Development division, Visakhapatnam, Andhra Pradesh 530047, India; jvprasad.008@gmail.com

* Correspondence: moriguch@che.kyutech.ac.jp

Academic Editor: Shujun Zhang

Received: 12 July 2017; Accepted: 8 August 2017; Published: 9 August 2017

Abstract: Two s-shaped polyaromatic dibenzo[c,l]chrysene derivatives have been synthesized by a two-step process, via. The Wittig reaction, followed by iodine, promoted photocyclization. These molecules have been characterized by ¹H NMR, FAB-MS, and elemental analysis. Further, the molecular structures of 4a and 4b have been confirmed by single crystal X-ray diffraction analysis. The protons located in the cove-regions of molecules 4a and 4b showed downfield shifts of the protons. Molecule 4a crystallized under the monoclinic system with space group *C2/c*, and the molecule 4b crystallized under the monoclinic system with space group *P2₁/n*. Molecules 4a and 4b showed strong absorption maxima wavelengths at 310 nm and 324 nm, respectively. The molar extinction coefficients (ϵ) of the compounds 4a and 4b indicated that molecule 4b has a better ability to absorb UV light than molecule 4a. The emission spectra of the molecules 4a and 4b displayed peaks in the region 429–456 nm. The shape of the UV-Visible and Fluorescence spectra of the molecules 4a and 4b look almost identical. However, molecule 4b exhibited better fluorescence intensity than molecule 4a. This may be due to the difference in the substituents of molecules 4a and 4b.

Keywords: Wittig reaction; photocyclization; dibenzo[c,l]chrysene; polyaromatic compounds; X-ray crystallography; UV-Visible absorption; fluorescence emission

1. Introduction

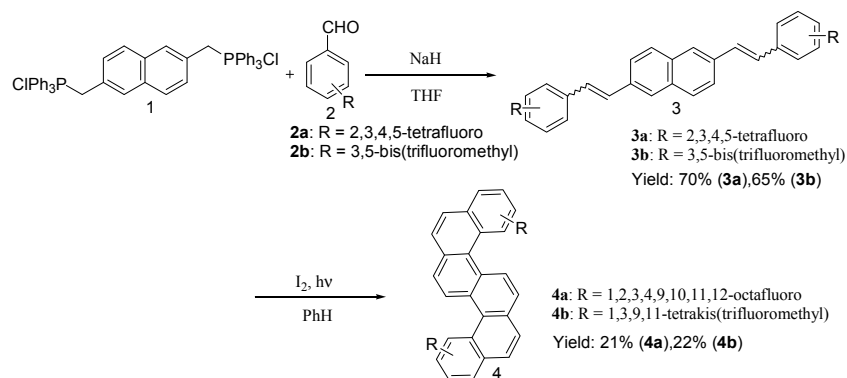
Polyaromatic hydrocarbons or π -conjugated materials are an important class of organic compounds because their important property of conductivity led to tremendous advancements in the field of organic electronics [1]. Over the past decade significant research has been done and the search for the new π -conjugated systems has been ongoing because of the important, rapidly growing number of applications in electronic devices such as semiconducting materials [2–5], organic solar cells [6], sensors [7], organic light-emitting diodes (OLEDs), organic field-effect transistors (OFETs), and flexible displays. π -conjugated materials have been extensively studied for their optoelectronic properties due to the offering of low-cost, large-area, and flexible electronic devices [8–10]. S-shaped dibenzo[c,l]chrysene derivatives are regarded as a hexacyclic polyaromatic hydrocarbon compound containing two cove-regions, and they have potential applications in biological systems and organic semiconductor materials [11,12]. The synthesis of s-shaped benzo[c,l]chrysene derivatives is of great interest, and is challenging because of the steric hindrance in the cove-regions. The synthesis of s-shaped

benzo[*c,l*]chrysene derivatives with substituents like -F, -CF₃ in the cove-region is even more challenging because of the increased steric hindrance. An ideal organic electronic material should have a low HOMO (highest occupied molecular orbital)-LUMO (lowest unoccupied molecular orbital) energy gap, good solid state packing, stability, solubility, and planarity. One of the fundamental principles in designing an air stable semiconducting material is incorporating electron withdrawing groups. It was reported that because of the incorporation of electron withdrawing groups, electron affinity of materials increases and the LUMO energy gap decreases; consequently, the band gap also decreases [13–15]. It was also reported that the introduction of fluorine atoms in the molecule increases the thermal stability of the molecule, which is important for the effective vapor-phase growth of the corresponding thin films [16]. Considering these basic principles, as part of our ongoing research objectives in this article we have investigated the synthesis, crystal structure, and photophysical properties of two fluorinated s-shaped polyaromatic compounds, which have the dibenzo[*c,l*]chrysene-like structure. We employed the typical Wittig and iodine-assisted photocyclization strategy for the synthesis of these molecules [17,18]. Earlier, we reported the synthesis of various kinds of polyaromatic compounds and evaluated their organic photoelectronic properties [19–22]. We believe that this study may be helpful to the material chemists in designing new materials with a view to achieve desired performance in devices and circuits.

2. Results and Discussion

Synthesis and Spectra Analysis

Molecules 4a and 4b have been synthesized in two steps. In the first step, 2,6-bis(triphenylphosphinomethyl)-naphthalene dichloride 1 was condensed with 2,3,4,5-tetrafluoro or 3,5-bis(trifluoromethyl) benzaldehyde (2a, 2b) via the Wittig reaction generated the precursors 3a and 3b. In the second step, 3a and 3b were subjected to iodine-assisted photocyclization, and yielded the corresponding s-shaped polyaromatic compounds 4a and 4b in moderate yields (Scheme 1).



Scheme 1. Schematic representation of synthesis of title compounds.

Molecules 4a and 4b have been characterized with ¹H NMR, EI-MS, and elemental analysis. ¹H NMR spectra for the photo-cyclized products 4a and 4b showed downfield shifts of the protons located in the cove-regions, which consist of four benzene rings. The five carbons in the cove-region were highlighted by using round circles in the molecular structures of 4a and 4b (Figures 1 and 2). The ¹H NMR shift values are 8.40 ppm for 4a, 8.65 ppm for 4b, respectively. The shifts were well explained by the strong ring current effects of the π-systems on the molecules.

Further to confirm the molecular structures of molecules 4a and 4b, good crystals suitable for the measurement of X-ray diffraction analysis were obtained by the slow evaporation of the dichloromethane solution using the slow diffusion method. The crystallographic details are summarized in Table 3. The compound 4a crystallizes with the monoclinic crystal system, space group C2/c. The molecular structure of 4a was depicted in Figure 1.

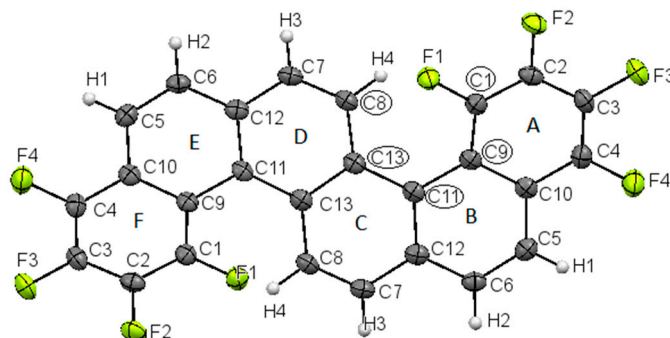


Figure 1. The molecular structure of **4a**; thermal ellipsoids were drawn on 50% probability level. Pale green ellipsoid represents F atoms.

The asymmetric unit of the title compound $C_{26}H_8F_8$, contains one-half of the formula unit. The dihedral angle between the planes of the end phenyl rings was quite large (59.85°). Three phenyl ring planes, A (defined by C1,C2,C3,C4,C9,C10), B (defined by C5,C6,C11,C12,C9,C10), and C (defined by C9,C10,C11,C12,C13,C13) were slightly leaned (Figure 1) and the plane angles between three phenyl rings are 10.56° for A–B, 18.89° for A–C, and 8.39° for B–C, respectively. The dihedral angles between the planes of the rings suggest that the shape of the molecule **4a** seems to be the planar, but it is a strained one. The steric hindrance due to the cove-region causes a deviation from the planarity of a molecule.

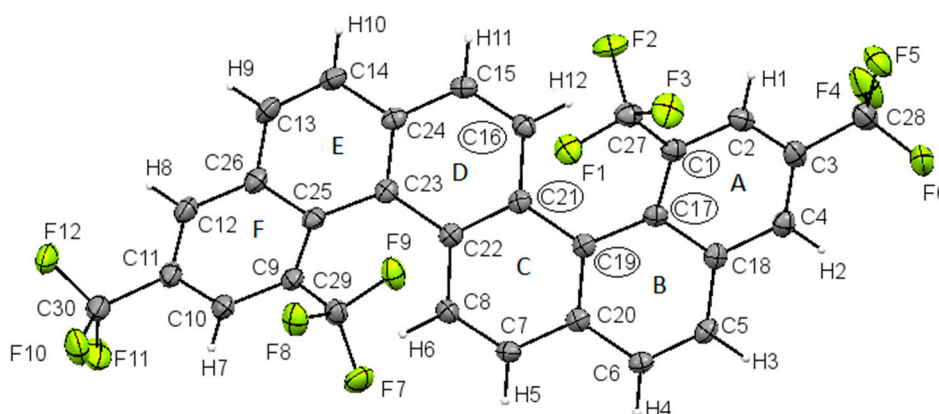


Figure 2. The molecular structure of **4b**; the thermal ellipsoids were drawn on 50% probability level. Pale green ellipsoid represents F atoms.

The compound **4b** also crystallizes with the monoclinic crystal system, space group $P2_1/n$. The molecular structure of molecule **4b** was depicted in Figure 2. The dihedral angle between the planes of the end phenyl rings was quite large (66.33°). Six phenyl ring planes, A (defined by C1,C2,C3,C4,C17,C18), B (defined by C5,C6,C17,C18,C19,C20), C (defined by C7,C8,C19,C20,C21,C22), D (defined by C15,C16,C21,C22,C23,C24), E (defined by C13,C14,C23,C24,C25,C26), and F (defined by C9,C10,C11,C12,C25,C26) were slightly leaned (Figure 2), and the plane angles between the six phenyl rings are 14.10° for A–B, 25.59° for A–C, 11.54° for B–C, 19.90° for C–D, 31.34° for C–E, 42.52° for C–F, 28.89° , 27.83° for B–E, and 66.33° for A–E, respectively. The dihedral angles between the planes of the rings suggest that the shape of the molecule **4b** seems to be planar, but it is a strained one. The dihedral angle between the planes of the aromatic rings of molecule **4b** is relatively more than molecule **4a**, because the bulky $-CF_3$ substituents in the cove-region causes more deviation from planarity. This suggests that molecule **4b** is more strained than molecule **4a**.

Crystal packing of the molecule **4a** was illustrated in Figure 3. In the crystal the molecules are assembled like planar geometry. Intermolecular short contacts of the molecule **4a** were listed in Table 1.

The ends of the molecules are linked by F...F, C-H...F short contacts. In between the layers, molecules are stacked by C-H...F, C...C and F...F short contacts, forming a flat, layer-like structure. In the packing diagram, molecular layers almost look like they are assembled parallel to each other.

Crystal packing of the molecule 4b was illustrated in Figure 4. Intermolecular short contacts of the molecule 4b were listed in Table 2. The molecular packing of the molecule 4b is not a planar one. Molecule 4b has a herring bone-like crystal packing system. In the crystal packing diagram, C-H...F, C...F, and F...F short contacts together generated three dimensional molecular networks.

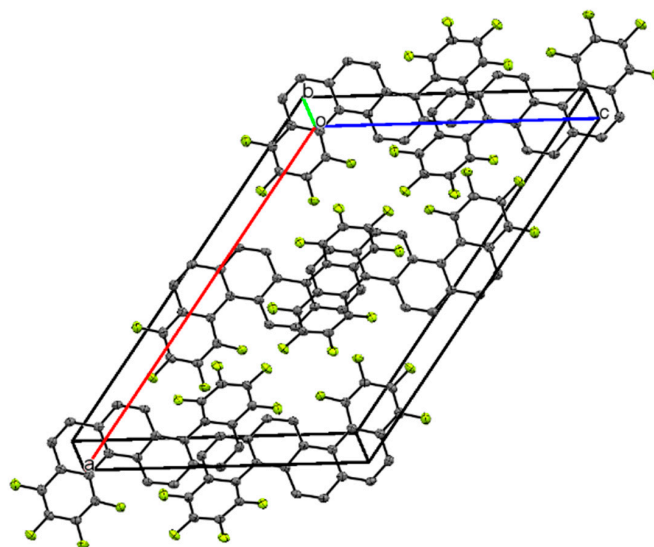


Figure 3. Molecular packing of the compound 4a and thermal ellipsoids are drawn on 50% probability level. Pale green ellipsoid represents F atoms.

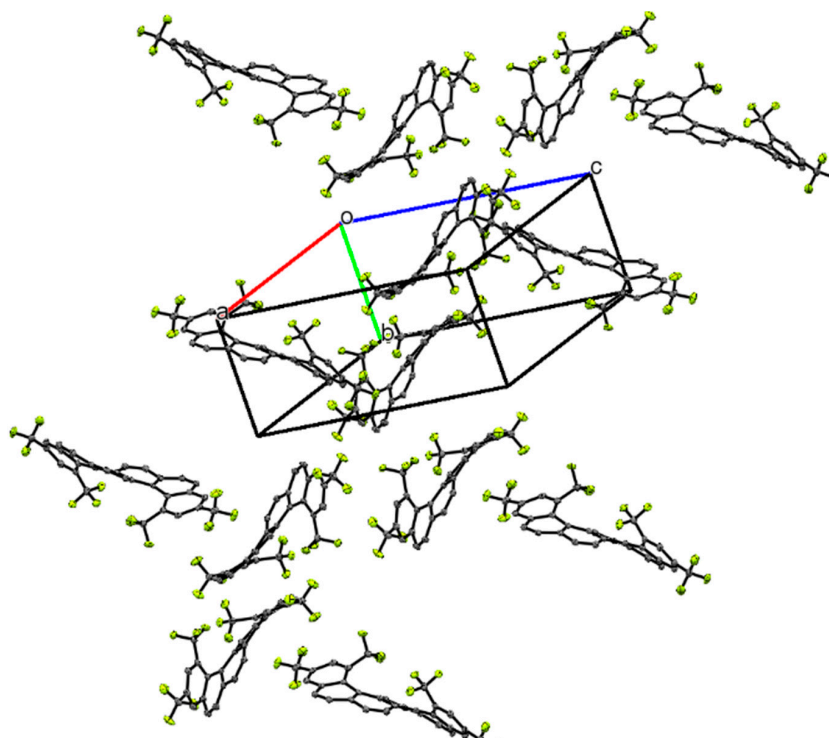


Figure 4. Molecular packing of the compound 4b along with a-axis, slightly bent towards front (thermal ellipsoids are drawn on 50% probability level). Pale green ellipsoid represents F atoms.

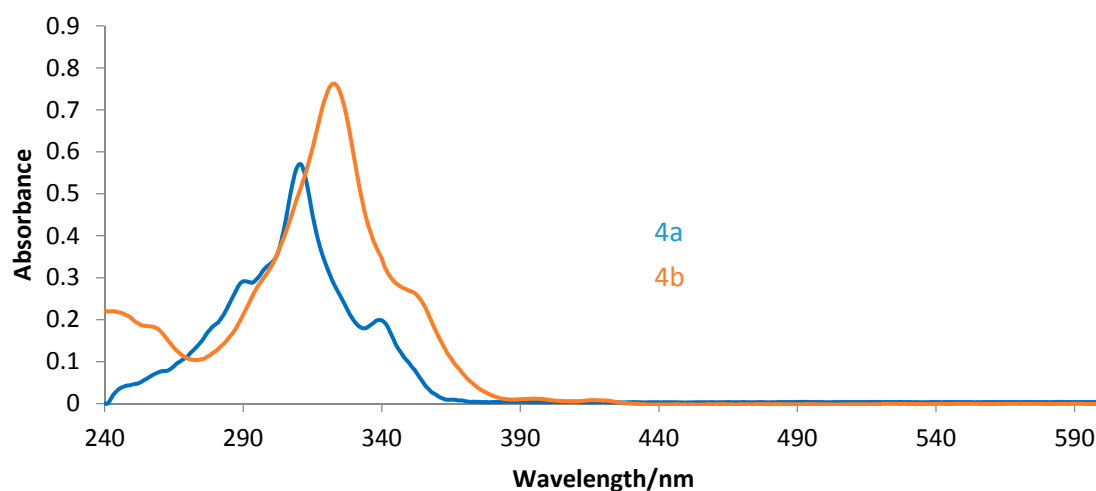
Table 1. Selected intermolecular short contacts (Å) of the molecule **4a**.

Short Contacts (between the Side Columns)		Short Contacts (between Molecules in the Column)	
F1–F4	2.862	C2–C11	3.327
F2–F2	2.918	C4–C8	3.252
H7–F1	2.525	C7–C9	3.324
F3–H8	2.565	F3–C4	3.147

Table 2. Selected intermolecular short contacts (Å) of the molecule **4b**.

Short Contacts (between the Side Columns)		Short Contacts (between Molecules in the Column)	
F4–F12	2.905		
H21–F5	2.6		
F2–F4	2.925	F9–C3	3.130
F4–F4	2.704		
F3–F3	2.882		
F1–F6	2.815		

Further to investigating the photophysical properties of molecules **4a** and **4b**, the UV-V is absorption and the Fluorescence emission of the molecules **4a** and **4b** were measured in a dichloromethane solution (1×10^{-5} mol/L), and their corresponding spectra were shown in Figures 5 and 6, respectively. The molecules **4a** and **4b** showed absorption maxima wavelength at 310 nm and 324 nm, respectively. The molar extinction coefficients (ϵ) of the compounds **4a** and **4b** were calculated as 5.7×10^4 (310 nm) and 7.5×10^4 (324 nm), $L \cdot mol^{-1} \cdot cm^{-1}$, respectively. These results indicate that molecule **4b** has better ability to absorb UV light than molecule **4a**. Because of the incorporation of the relatively strong electron withdrawing $-CF_3$ group in molecule **4b**, the band gap between HOMO, LUMO of **4b** (3.82 eV) is less than that of molecule **4a** (3.98 eV). As a result of this, more molecules of **4b** absorb energy than those of molecule **4a**. This improves the excitation charge transfer and transport of **4b** than **4a**.

**Figure 5.** UV-Visible absorption spectra of molecules **4a** and **4b**.

The emission spectra of the molecules **4a** and **4b** were recorded in dichloromethane solution (1×10^{-5} mol/L), and their emission spectra is shown in Figure 6. Emission spectra of the complexes were measured by exciting the complexes at their absorption maxima wavelengths 310 nm and 324 nm, respectively. The emission spectra of molecules **4a** and **4b** displayed peaks in the region 429–456 nm. The strong emissions can be explained by the molecular shapes of the compounds **4a** and **4b**. In another words, the compounds have no flexible parts; therefore, the excited energy cannot be relaxed through

molecular vibrations. The shape of the emission spectrum of both the molecules almost looks identical. However, the molecule 4b displayed relatively higher fluorescence intensity than molecule 4a. This may be due to the difference in the substituents of molecules 4a and 4b. Also, because of the more strained geometry of molecule 4b, relatively more energy will be used for the charge redistribution in the excited state than for molecule 4a.

HOMO and LUMO energy level calculations of the π systems of the compounds were carried out using density functional theory (DFT) B3LYP 6-31G(d) level on SPARTAN16 Suite program [23]. Atomic coordinate data (x, y, z) of the X-ray analysis were used in the calculations. The calculation results were HOMO -5.91eV , LUMO -1.93eV for 4a and HOMO -6.05eV , and LUMO -2.23eV for 4b, respectively (Figure 7). The energy gaps were 3.98eV for 4a and 3.82eV for 4b.

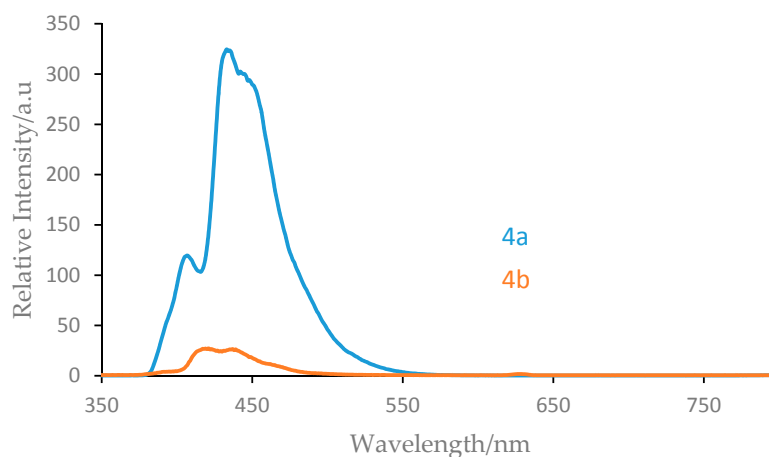


Figure 6. Emission spectra of the molecules 4a and 4b.

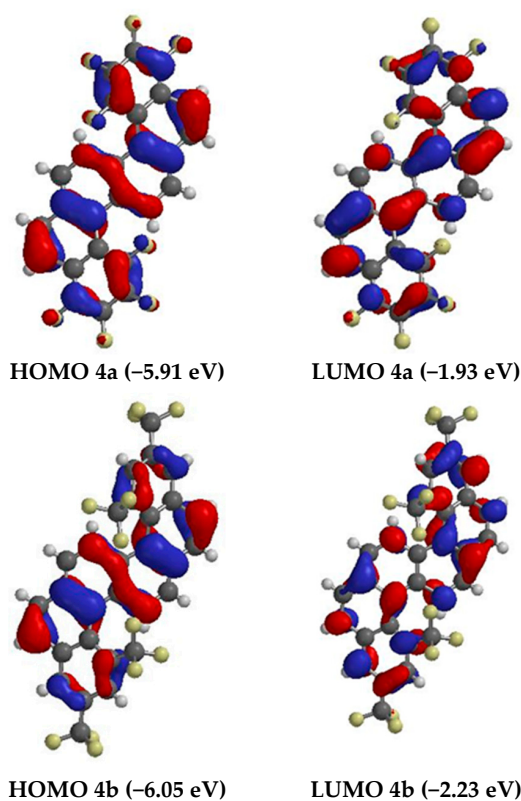


Figure 7. HOMO and LUMO orbitals in the crystals of the compounds 4a and 4b.

3. Experiments

3.1. Materials and Instrumentation

All reagents and solvents were obtained from commercial sources and used without further purification. The ^1H NMR spectra were recorded on a Bruker AVANCE400S spectrometer (Bruker, Yokohama, Japan) in CDCl_3 with tetramethylsilane (Me_4Si) as an internal reference. The positive fast atom bombardment (FAB) mass spectrum (MS) of the complex were obtained on a Nippon Densi JEOL JMS-SX102A spectrometer (JEOL, Tokyo, Japan) using NBA (nitrobenzylalcohol) as the matrix and DCM (dichloromethane) as the solvent. The instrument was operated in positive ion mode over an m/z range of 100–2000. Elemental analysis data were recorded on a Yanako MT-4 analyzer. A JASCO V-550 spectrophotometer (Yanako group, Kyoto, Japan) was used for obtaining UV-Vis spectra in dichloromethane with a 250–900 nm range. The HITACHI F-2500 spectrophotometer (Hitachi High-Technologies Corporation, Tokyo, Japan) was used for fluorescence spectra measurements in dichloromethane with a 250–900 nm range. CCDC no. 1551483 and 1551484 contain the supplementary crystallographic data for the complexes 4a and 4b, respectively.

3.2. Synthesis

3.2.1. Experimental procedure for the synthesis of molecules 3a and 3b

2,6-Bis(triphenylphosphinomethyl)-naphthalene dichloride Wittig Salt (0.75 g, 1.0 mmol) 1 and NaH (72 mg, 3 mmol) were taken in 200 mL of dry THF in a round-bottom flask under argon stream. To this, 2,3,4,5-tetrafluoro (or) 3,5-bis(trifluoromethyl) benzaldehyde (2.0 mmol) 2 was added drop-wise, the mixture was stirred for 14 h, quenched with 1.0% HCl aq., and extracted twice with CH_2Cl_2 . The organic layers were washed once with 50 mL water, twice with 50 mL of brine solution, dried over MgSO_4 , and then the solvent was removed under reduced pressure. The precursors 3a and 3b were obtained using silica gel (Wako gel C-300) column chromatography (330 mg, 70% yield for 3a, 390 mg, 65% yield for 3b) with CH_2Cl_2 as an eluent.

3.2.2. Typical Procedure for the Photo Cyclization of the Compounds 4a and 4b

4,9-Bis{2'-(2,3,4,5-tetrafluoro or 3,5-bis(trifluoromethyl) phenyl)ethenyl}-naphthalene (1.0 mmol) 3 was dissolved in 200 mL of benzene in a round-bottom flask. To this iodine (10 mmol) was added, the mixture was stirred and irradiated UV light using high-pressure Hg lamp for 14 h, quenched with 1.0 mol/L $\text{Na}_2\text{S}_2\text{O}_3$ solution, allowed to warm to room temperature, and extracted twice with ethyl acetate. The organic layers were washed once with 50 mL water, twice with 50 mL of brine solution, dried over MgSO_4 , and then the solvent was removed under reduced pressure. The title compound was obtained using silica gel (Wako gel C-300) column chromatography (100 mg, 21% yield for 4a, 130 mg, 22% for 4b) with CH_2Cl_2 as an eluent.

3.2.3. Analytical Data for Compounds 4a and 4b

4a Mp: 257–263 °C; ^1H NMR (400 MHz, CDCl_3): 8.40 (d, 2H, $J = 7.82\text{Hz}$), 8.25 (d, 2H, $J = 10.1\text{ Hz}$), 8.01 (d, 2H, $J = 8.76\text{ Hz}$), 7.92 (d, 2H, $J = 9.08\text{ Hz}$); EI-MS: m/z 472 (M^+); Elemental Analysis: $\text{C}_{26}\text{H}_8\text{F}_8$, Found: C: 65.99%, H: 1.61%, Calculated: C: 66.11%, H: 1.71%.

4b Mp.: 268–271 °C; ^1H NMR (400 MHz, CDCl_3): 8.65 (d, 2H, $J = 8.93\text{ Hz}$), 8.45 (s, 2H), 8.23 (s, 2H), 7.95 (d, 4H), 7.84 (d, 2H, $J = 8.68\text{ Hz}$); EI-MS: m/z 600 (M^+); Elemental Analysis: $\text{C}_{30}\text{H}_{12}\text{F}_{12}$, Found: C: 59.84%, H: 2.35%, Calculated: C: 60.01%, H: 2.01%.

3.3. Data Collection, Refinement, and Structural Determination

Single crystals of compounds 4a and 4b were obtained from a solution of dichloromethane at room temperature using the slow diffusion method. The crystallographic data of these complexes were summarized in Table 3. APEX2 software was used for the preliminary determination of the unit

cell [24]. The determination of the integrated intensities and unit cell refinement were performed using SAINT program [25]. The structures were solved with SHELXL-2014/7, and subsequent structure refinements were performed with SHELXL-2014/7 [26].

Table 3. Crystal data and structure refinements for 4a and 4b.

Parameters Measured	4a	4b
Empirical Formula	C ₂₆ H ₈ F ₈	C ₃₀ H ₁₂ F ₁₂
Formula Weight (g·mol ⁻¹)	472.32	600.40
Crystal shape, color	Prism, yellow	Prism, yellow
Temperature	120 K	120 K
Radiation type	Mo K α	Mo K α
Wavelength (Å)	0.7107	0.7107
Crystal system	Monoclinic	Monoclinic
Space group	C2/c	P2 ₁ /n
Unit cell dimensions	a = 20.615(4) Å b = 7.3711(13) Å c = 14.044(3) Å $\alpha = 90^\circ$ $\beta = 124.2960(10)^\circ$ $\gamma = 90^\circ$	a = 15.779(3) Å b = 8.0502(15) Å c = 18.327(3) Å $\alpha = 90^\circ$ $\beta = 96.565(2)^\circ$ $\gamma = 90^\circ$
Volume	1763(5) Å ³	2312.8(7) Å ³
Z	4	4
Calculated density (Mg·m ⁻³)	1.779	1.724
Absorption coefficient mm ⁻¹	0.162	0.168
F(000)	944	1200
Crystal Size (mm)	0.25 × 0.15 × 0.10	0.40 × 0.25 × 0.15
Theta range for data collection	2.39 to 24.99°	1.61 to 25.03°
Limiting indices	-24 < h < 24 -8 < k < 8 -16 < l < 16	-18 < h < 18 -9 < k < 9 -21 < l < 21
Reflections collected/unique	8044/1548 [Rint = 0.233]	21481/4070 [Rint = 0.304]
Completeness to theta (%)	99.9	99.6
Max. and min. transmission	0.984 and 0.864	0.975 and 0.717
Refinement method	Full-matrix LS on F ²	Full-matrix LS on F ²
Data/restraints/parameters	1548/108/154	4070/0/379
Goodness-of-fit on F ²	1.073	1.128
Final R indices [I > 2 sigma (I)]	R1 = 0.0346 wR2 = 0.0983	R1 = 0.0299 wR2 = 0.0800
R indices (all data)	R1 = 0.0410 wR2 = 0.1034	R1 = 0.0345 wR2 = 0.0943
Largest diff. peak and hole	0.276 and -0.188	0.239 and -0.290

4. Conclusions

In conclusion, we have reported the synthesis of two s-shaped fluorinated polyaromatic organic materials. These molecules were characterized by ¹H NMR, EI-MS, and elemental analysis. The protons located in the cove-regions of molecules 4a and 4b showed downfield shifts of the protons. The molecular structures of molecules 4a and 4b were determined by X-ray diffraction analysis. Molecules 4a and 4b have different crystal packing. Furthermore, molecules 4a and 4b showed strong absorption maxima at wavelengths 310 nm and 324 nm, respectively. The molar extinction coefficients (ϵ) indicated that molecule 4b (7.5×10^4 L·mol⁻¹·cm⁻¹) has a better ability to absorb UV light than molecule 4a (5.7×10^4 L·mol⁻¹·cm⁻¹). The emission spectra of molecules 4a and 4b displayed peaks

in the region 428–456 nm. However, molecule 4b exhibited better fluorescence intensity than molecule 4a. This may be due to the difference in the substituents of molecules 4a and 4b.

Acknowledgments: We are grateful to the Center for Instrumental Analysis, Kyushu Institute of Technology (KITCIA) for EI-MS, ¹H NMR spectral measurements, elemental analyses and single crystal X-ray measurements. This research was financially supported by JSPS KAKENH Grant Number 15K05611.

Author Contributions: Tetsuji Moriguchi conceived and designed the experiments. Daichi Tabuchi and Venkataprasad Jalli performed the experiments. Venkataprasad Jalli and Daisuke Yakeya analyzed the data. Akihiko Tsuge contributed reagents/materials/analysis tools. Tetsuji Moriguchi prepared the manuscript.

Conflicts of Interest: The authors declare no conflicts of interest.

References

1. Wang, C.; Dong, H.; Hu, W.; Liu, Y.; Zhu, D. Semiconducting π -Conjugated Systems in Field-Effect Transistors: A Material Odyssey of Organic Electronics. *Chem. Rev.* **2012**, *112*, 2208–2267. [[CrossRef](#)] [[PubMed](#)]
2. Anthony, J.E. Functionalized Acenes and Heteroacenes for Organic Electronics. *Chem. Rev.* **2006**, *106*, 5028–5048. [[CrossRef](#)] [[PubMed](#)]
3. Blouin, N.; Leclerc, M. Poly(2,7-carbazole)s: Structure–Property Relationships. *Acc. Chem. Res.* **2008**, *41*, 1110–1119. [[CrossRef](#)] [[PubMed](#)]
4. Pron, A.; Gawrys, P.; Zagorska, M.; Djurado, D.; Demadrille, R. Electroactive materials for organic electronics: Preparation strategies, structural aspects and characterization techniques. *Chem. Soc. Rev.* **2010**, *39*, 2577–2632. [[CrossRef](#)] [[PubMed](#)]
5. Wu, W.; Liu, Y.; Zhu, D. π -Conjugated molecules with fused rings for organic field-effect transistors: Design, synthesis and applications. *Chem. Soc. Rev.* **2010**, *39*, 1489–1502. [[CrossRef](#)] [[PubMed](#)]
6. Lin, Y.; Li, Y.; Zhan, X. Small molecule semiconductors for high-efficiency organic photovoltaics. *Chem. Soc. Rev.* **2012**, *41*, 4245–4272. [[CrossRef](#)] [[PubMed](#)]
7. Sokolov, A.N.; Roberts, M.E.; Bao, Z. Graphene speeds up computers: Carbon. *Mater. Today* **2009**, *12*, 12. [[CrossRef](#)]
8. Aleshin, A.N.; Lee, J.Y.; Chu, S.W.; Kim, J.S.; Park, Y.W. Mobility studies of field-effect transistor structures based on anthracene single crystals. *Appl. Phys. Lett.* **2004**, *84*, 5383. [[CrossRef](#)]
9. Kelley, T.W.; Boardman, L.D.; Dunbar, T.D.; Muires, D.V.; Pellerite, M.J.; Smith, T.Y.P. High-Performance OTFTs Using Surface-Modified Alumina Dielectrics. *J. Phys. Chem. B* **2003**, *107*, 5877–5881. [[CrossRef](#)]
10. Garnier, F.; Yassar, A.; Hajlaoui, R.; Horowitz, G.; Deloffre, F.; Servet, B.; Ries, S.; Alnot, P. Molecular engineering of organic semiconductors: Design of self-assembly properties in conjugated thiophene oligomers. *J. Am. Chem. Soc.* **1993**, *115*, 8716–8721. [[CrossRef](#)]
11. Sharma, A.K.; Lin, J.-M.; Desai, D.; Amin, S. Convenient Syntheses of Dibenzo[c,p]chrysene and Its Possible Proximate and Ultimate Carcinogens: In Vitro Metabolism and DNA Adduction Studies. *J. Org. Chem.* **2004**, *70*, 4962–4970. [[CrossRef](#)] [[PubMed](#)]
12. Brison, J.; De Bakker, C.; Defay, N.; Geerts-Evrard, F.; Marchant, M.-J.; Martin, R.H. Synthèse Photochimique D'Hydrocarbures Polycycliques Aromatiques et Étude en RMN-¹H Des Protons de Baie. Effets de Solvant Spécifiques et Effets Nucleaires Overhauser. *Bulletin des Sociétés Chimiques Belges* **1983**, *92*, 901–912. [[CrossRef](#)]
13. Swartz, C.R.; Parkin, S.R.; Bullock, J.E.; Anthony, J.E.; Mayer, A.C.; Malliaras, G.G. Synthesis and Characterization of Electron-Deficient Pentacenes. *Org. Lett.* **2005**, *7*, 3163–3166. [[CrossRef](#)] [[PubMed](#)]
14. Kikuzawa, Y.; Mori, T.; Takeuchi, H. Synthesis of 2,5,8,11,14,17-Hexafluoro-hexa-*peri*-hexabenzocoronene for n-Type Organic Field-Effect Transistors. *Org. Lett.* **2007**, *9*, 4817–4820. [[CrossRef](#)] [[PubMed](#)]
15. Song, D.; Wang, H.B.; Zhu, F.; Yang, J.L.; Tian, H.K.; Geng, Y.H.; Yan, D.H. Phthalocyanato Tin(IV) Dichloride: An Air-Stable, High-Performance, n-Type Organic Semiconductor with a High Field-Effect Electron Mobility. *Adv. Mater.* **2008**, *20*, 2142–2144. [[CrossRef](#)]
16. Hakan, U.; Facchetti, A.; Tobin, J.M. n-Channel Semiconductor Materials Design for Organic Complementary Circuits. *Acc. Chem. Res.* **2011**, *44*, 501–510.
17. Liu, J.; Ma, J.; Zhang, K.; Ravat, P.; Machata, P.; Avdoshenko, S.; Hennersdorf, F.; Komber, H.; Pisula, W.; Weigand, J.J.; et al. π -Extended and Curved Antiaromatic Polycyclic Hydrocarbons. *J. Am. Chem. Soc.* **2017**, *139*, 7513–7521. [[CrossRef](#)] [[PubMed](#)]

18. Olena, P.; Vladimir, A.A.; Alexey, A.G.; Frank, H.; Frank, W.H.; Konstantin, Y.A. Synthesis of Rationally Halogenated Buckybowls by Chemoselective Aromatic C–F Bond Activation. *Angew. Chem. Int. Ed.* **2017**, *56*, 4834–4838.
19. Nagamatsu, S.; Moriguchi, T.; Nagase, T.; Oku, S.; Kuramoto, K.; Takashima, W.; Okauchi, T.; Mizoguchi, K.; Hayase, S.; Kaneto, K. A steady operation of n-type organic thin-film transistors with cyano-substituted distyrylbenzene derivative. *Appl. Phys. Express* **2009**, *2*, 1–3. [[CrossRef](#)]
20. Nagamatsu, S.; Oku, S.; Kuramoto, K.; Moriguchi, T.; Takashima, W.; Okauchi, T.; Hayase, S. Long-Term Air-Stable n-Channel Organic Thin-Film Transistors Using 2,5-Difluoro-1,4-phenylene-bis[2-[4-(trifluoromethyl)phenyl]acrylonitrile]. *Appl. Mater. Interfaces* **2014**, *6*, 3847–3852. [[CrossRef](#)] [[PubMed](#)]
21. Moriguchi, T.; Kitou, N.; Prasad, J.V.; Yoza, K.; Nagamatsu, S.; Okauchi, T.; Tsuge, A.; Takashima, W. Molecular structures of n-type semiconducting material 2,5-difluoro-1,4-phenylene-3,3-bis[2-[(4-trifluoromethyl)phenyl]acrylonitrile] and its photo dimerization product. *J. Mol. Struct.* **2016**, *1118*, 372–377. [[CrossRef](#)]
22. Moriguchi, T.; Higashi, M.; Yakeya, D.; Prasad, J.V.; Tsuge, A.; Okauchi, T.; Nagamatsu, S.; Takashima, W. Synthesis, characterization and air stable semiconductor properties of thiophene-condensed pyrene derivatives. *J. Mol. Struct.* **2017**, *1127*, 413–418. [[CrossRef](#)]
23. Yamamoto, T.; Komarudin, D.; Arai, M.; Lee, B.-L.; Suganuma, H.; Asakawa, N.; Inoue, Y.; Kubota, K.; Sasaki, S.; Fukuda, T.; et al. Extensive Studies on π -Stacking of Poly(3-alkylthiophene-2,5-diyl)s and Poly(4-alkylthiazole-2,5-diyl)s by Optical Spectroscopy, NMR Analysis, Light Scattering Analysis, and X-ray Crystallography. *J. Am. Chem. Soc.* **1998**, *120*, 2047–2058. [[CrossRef](#)]
24. *APEX2 Version 2009.9*; Bruker AXS Inc.: Tokyo, Japan, 2009.
25. *SAINT Version 7*; Bruker AXS Inc.: Tokyo, Japan, 2009.
26. Sheldrick, G.M. A short history of SHELX. *Acta Cryst.* **2008**, *A64*, 112–122. [[CrossRef](#)] [[PubMed](#)]



© 2017 by the authors. Licensee MDPI, Basel, Switzerland. This article is an open access article distributed under the terms and conditions of the Creative Commons Attribution (CC BY) license (<http://creativecommons.org/licenses/by/4.0/>).